Revision 1

The interplay between twinning and cation inversion in $MgAl_2O_4$-spinel: Implications for a nebular thermochronometer

Authors: Venkateswara Rao Manga[1,2], Krishna Muralidharan[1,2], Thomas J. Zega[1,2]

Affiliations:

[1]Lunar and Planetary Laboratory
University of Arizona
1629 E. University Blvd.
Tucson AZ 85721.

[2]Department of Materials Science and Engineering
1235 E. James E. Rogers Way
University of Arizona
Tucson AZ 85721.

Send correspondence to Venkateswara Rao Manga (email: manga@email.arizona.edu)
520-780 7759.

Keywords: spinel twins, cation inversion, thermodynamics, order parameter, nebular thermochronometer

This is the peer-reviewed, final accepted version for American Mineralogist, published by the Mineralogical Society of America.
The published version is subject to change. Cite as Authors (Year) Title. American Mineralogist, in press.
DOI: https://doi.org/10.2138/am-2021-7874. http://www.minsocam.org/

Abstract

We report a first-principles-based thermodynamic investigation of the interplay between cation inversion and twinning in $MgAl_2O_4$ spinel (MAS). We examine the atomic-scale structure of (111) twins and characterize the local octahedral and tetrahedral distortions. We observe that the asymmetric nature of polyhedral distortions about the (111) twin plane causes anisotropy in cation inversion energies near the planar fault. The predicted enthalpies and entropies of inversion reveal that in comparison to the Kagome layer, the anti-site occupancies of Al and Mg, i.e., cation inversion, on the mixed-cation-layer near the twin boundary are more favorable and stable in the entire range of temperature of twin stability. Structurally, such a stable inversion is necessitated by the minimization in the polyhedral distortions, especially by the octahedral distortion, which exhibits a reduction of four orders of magnitude relative to the polyhedra with no inversion. The fundamental understanding obtained on the thermodynamics of the twin-cation inversion interplay in conjunction with the kinetics of inversion was used as a basis for developing a thermochronometer for deducing the temperature of twinning in MAS. This work serves as an important steppingstone for experimental characterization of MAS structures within a host of earth and planetary materials. In the case of the latter, our results enable the use of planar faults, such as twins, as important markers for deducing the physical and chemical landscape that MAS experienced in its evolution and transport within the solar protoplanetary disk.

1. Introduction

Magnesium aluminate spinel (MAS) $MgAl_2O_4$ finds interest across scientific fields owing to its technological, geological, and astrophysical relevance (Ganesh 2013; Biagioni and Pasero 2014; Parisi et al. 2014; Bosi et al. 2016). The crystal chemistry and the underlying thermodynamics of spinel materials has therefore, received considerable attention for decades (e.g., Navrotsky and Kleppa 1967; Méducin et al. 2004). In planetary science, MAS is a significant phase (Brearely and Jones 1998). It occurs as a constituent mineral in calcium-aluminum-rich inclusions (CAIs) (MacPherson 2014), which are the first solids to have condensed in our early solar nebula (Amelin et al. 2002; Connelly et al. 2012). Consequently, the mineralogy and the crystal chemistry of MAS as well as other phases in CAIs is important for understanding their origins and physical processes of the early solar nebula.

This is the peer-reviewed, final accepted version for American Mineralogist, published by the Mineralogical Society of America.
The published version is subject to change. Cite as Authors (Year) Title. American Mineralogist, in press.
DOI: https://doi.org/10.2138/am-2021-7874. http://www.minsocam.org/

An interesting feature of MAS crystal chemistry is the way in which its Al and Mg cations populate its crystallographic sites within its cubic structure (space group: Fd-3m) as a function of temperature. These cations can disorder, which occurs when the Al atoms substitute into tetrahedral sites normally occupied by Mg, whereas Mg substitutes into octahedral sites normally occupied by Al. This process is referred to as inversion, and the inversion reaction Al(M) + Mg(T) = Mg(M) + Al(T), where M = the octahedral site and T = the tetrahedral site, is thermally activated (O'Neill and Navrotsky 1984; Kashii et al. 1999; Redfern et al. 1999). At 1 atm pressure, inversion was shown to occur at temperatures > ~300 K and reaches a value of x = ~0.37 in $(Mg_{1-x}Al_x)^T(Al_{2-x}Mg_x)^MO_4$ at 2000 K (Navrotsky and Kleppa 1967; Méducin et al. 2004). Given that MAS grains in CAIs and possibly other planetary materials could have experienced large-scale transport within the solar protoplanetary disk (Ciesla 2007, 2009; Brownlee 2014) and hence a wide range of thermodynamic conditions, it is important to understand the extent of inversion as a function of temperature and pressures relevant to the early solar nebula. Such information is currently unavailable and represents an important and relevant knowledge gap.

Cation disorder in MAS is also sensitive to structural perturbations in the form of planar faults (Rasmussen et al. 2011), which can include twin planes within the phase. Twins can occur during deformation, phase transitions or crystal growth and are named accordingly as deformation twins, phase transition twins or growth twins. The twin plane is denoted by the (hkl) crystallographic plane parallel to which the twin occurs and demarcates the planar fault that divides twin domains from each other. As a coherent interface between the two twin domains whose lattice vectors are inclined to each other at a specific angle, these twin planes are energetically unfavorable in terms of their formation energies. As a result, these faults tend to minimize their energies by rearranging their local atomic structure and chemistry as a function of the imposed thermodynamic conditions, i.e., pressure, temperature, and chemical potential. The exact nature and extent of the atomic rearrangement within the MAS twin remains an open question in the mineral and materials sciences (Hornstra 1960). In $CaTiO_3$, which is a nonferroelectric material, twin planes were reported to be ferrielectric (Goncalves-Ferreira et al. 2008).

Twins in MAS that occur parallel to the (111) plane form from a faulty stacking sequence in the cubic close-packed (ccp) oxygen sublattice with or without any changes to the cation sublattices. The atomic structure of (111) twins can be described as a hexagonal close packed (hcp) oxygen (ABA stacking) sublattice in an otherwise cubic-close-packed (ccp) sublattice of oxygen

(ABCABC…) (Hornstra 1960). The local atomic structure near the stacking faults was first examined by Hornstra (Hornstra 1960) based on the crystallographic theory of dislocations. Hornstra showed that twins can be generated by the glide of super-partial dislocations on the (111) plane and proposed two structural models. Twins in MAS can also occur during crystal growth by developing a faulty stacking sequence of oxygen layers in its cubic close-packed arrangement (ABCABC… stacking sequence). However, in neither of the models proposed by Hornstra is the interplay between twin boundary and the cation disorder in its vicinity considered and this must be taken into account as shown by recent experimental and simulation work (Rasmussen et al. 2011; Uberuaga and Perriot 2020) that focused on other types planar faults. For example, MAS (100) surfaces, which are a particular type of planar faults, were found to exhibit inversion that is in stark contrast to the bulk spinel. Rasmussen et al. (2011) reported a stable cation-inversion on the Al/O-rich (100) surface of MAS employing non-contact atomic force microscopy (NC-AFM) and surface x-ray diffraction (SXRD) in conjunction with first-principles calculations. They reported that the identified stable inversion is driven by the charge distribution that takes place at the surface. However, there has not been much effort dedicated towards understanding the evolution in inversion-driven complexion in the vicinity of twin planes. The lack of insight into the complex twin-disorder interplay especially as a function of temperature represents yet another knowledge gap. Such faults, in conjunction with a quantitative assessment of the associated Al/Mg disorder, has the potential to reveal the temperature-locus of physical processes such as deformation, shock, and crystal growth in the disk to which the MAS was subjected.

Keeping the identified knowledge gaps in mind, we carry out density-functional theory (DFT)-driven investigations within a thermodynamic modeling framework for deducing the temperature-dependent interplay between twins and the extent of cation disorder in MAS systems that are typically found in planetary materials. Using DFT, we explicitly calculate entropic contributions to the Gibbs free energies, enabling an accurate description of the temperature-driven inversion-twin interplay in MAS. Such results are especially relevant in an era where direct atomic-resolution imaging of materials in aberration-corrected electron microscopes has been realized (Krivanek et al. 2010; Pennycook 2017). The developed thermodynamic model in conjunction with the kinetics of cation disorder is utilized to make a thermochronometer for deducing the temperature of twinning in MAS found in planetary materials, including CAIs, in addition to serving as a valuable

self-consistent framework for constraining the thermodynamic landscape underlying the solar nebula.

2. Methods

First-principles DFT calculations were carried out using Viennna Ab initio Simulation Package (VASP) employing the projector augmented wave (PAW) method (Kresse and Furthmüller 1996). The exchange correlation functional as described by Purdew-Burke-Ernzerhof (PBE) (Perdew and Zunger 1981; Perdew et al. 1996) is used in the calculations. Supercells containing 336 atoms are used to calculate the twin-formation energies and the thermodynamics of inversion with a plane wave cutoff energy of 520 eV and Gamma-centered kmesh of 4x4x2. We performed the calculations for bulk pristine structures and twin-containing structures in order to predict the energetics of inversion in the vicinity of the twin planes. The (111) twins in spinel are generated by a 180°-rotation of one half of the crystal with respect to the other half about the [111]-axis. The twin-formation energy is obtained as E(prist)-E(twin)/2A, where E(prist) is the energy of the pristine supercell and E(twin) is the energy of the supercell with two twin planes of an area 2A. The two twin planes in the supercell are separated by 14.459 Å (see supplementary information). Supercells with more than 336-atoms may offer better isolation of the twin planes from each other, especially, to investigate the polarity and the inversion near the fault. The thermodynamic driving force for inversion near the twin plane is expressed as the change in twin-formation energy due to the inversion at the twin plane. Hence, if the dispersion contributions due to twin-associated polarization are assumed to be nearly constant as a function of percentage of inversion, the thermodynamic driving force for inversion near the twin plane is accurate due to subtracted dispersion effects. In addition, to investigate the stable cation configurations at finite temperatures, the entropic contributions to the Gibbs free energies are predicted using the Debye-Gruneisen (DG) approach (Slater 1939; Dugdale and MacDonald 1953). The ground state equation of state is calculated to obtain the properties that are required to predict the Debye temperature of spinel with and without a twin. A Birch-Murnaghan equation of state is used to fit the energy-volume data (Birch 1947, 1978). Prediction of vibrational entropy from phonons is prohibitively intensive due to large supercell sizes required by the twin calculations. However, the calculated phonon density of states of pristine $MgAl_2O_4$ spinel is used to estimate the second moment Debye temperature, which compares accurately with the obtained Debye temperature from the DG approach. The

This is the peer-reviewed, final accepted version for American Mineralogist, published by the Mineralogical Society of America.
The published version is subject to change. Cite as Authors (Year) Title. American Mineralogist, in press.
DOI: https://doi.org/10.2138/am-2021-7874. http://www.minsocam.org/

supplementary information provides the DG formalism and the procedure to estimate the thermodynamic properties from the first-principles predicted equations of state of supercells with and without the (111) twin.

3. Results

The crystal structure and atomic packing along the [111]-direction in a pristine MAS with no inversion on the cation sublattices (the oxygen atoms at the corners of the polyhedra are not shown for clarity) is depicted in Figure 1. Mg and Al cations are tetrahedrally and octahedrally coordinated, respectively, with oxygen. Along the [111] direction, the cation layers of pure Al and Al+Mg are arranged alternatively between the oxygen layers (which are marked as ABCABC…). The pure Al-layer (marked as O^{K}_{Al}) is also referred to as the 'Kagome' layer, which is a Japanese word for the structural pattern exhibited by this layer (O'Keefe and Hyde 1997). The Al+Mg-layer (marked with T^{I}_{Mg}, O^{I}_{Al} and T^{II}_{Mg}) is the mixed-cation layer.

Figure 2 shows the structure of spinel with a (111) twin and the polyhedral distortions within its local vicinity. The distortions of Al-O octahedra and Mg-O tetrahedra especially in vicinity of the (111) twin plane, are analyzed employing octahedral and tetrahedral distortion parameters. We quantify the distortions via:

$$\Delta\, d_n = 1/n \sum_{i=1}^{n} \frac{R-\bar{R}}{\bar{R}} \quad (1)$$

where Δd is the polyhedral distortion parameter; R is the individual metal (M) to oxygen (O) bond length (M-O) in the (MO)n polyhedron; and $\bar{R}$ is the mean M-O bond length in the (MO)n polyhedron. With n = 6, Δd_0 is the octahedral distortion parameter, whereas with n = 4, Δd_t is the tetrahedral distortion parameter.

The distortion parameters of AlO_6- and MgO_4- polyhedra on each side of the twin plane are also shown in Figure 2. The layer marked '$T_{Mg}^{I-t} + O_{Al}^{I-t} + T_{Mg}^{II-t}$' is the mixed-cation layer near the twin boundary (Fig. 2a, red font and annotation). This mixed-cation layer exhibits the highest strain and distortion in terms of Δd_0, Δd_t, (Fig. 2b) as well as $\bar{R}$ (not shown on the figure). The AlO_6 octahedra and the MgO_4-tetrahedra in the mixed layer exhibit expansion (with $\bar{R}_{Al-O}$ of 2.01

This is the peer-reviewed, final accepted version for American Mineralogist, published by the Mineralogical Society of America.
The published version is subject to change. Cite as Authors (Year) Title. American Mineralogist, in press.
DOI: https://doi.org/10.2138/am-2021-7874. http://www.minsocam.org/

Å) and contraction (with $\bar{R}_{Mg-O}$ of 1.907 Å), respectively, in comparison to the $\bar{R}_{Al-O}$ of 1.937 and $\bar{R}_{Mg-O}$ of 1.943 Å in the pristine bulk spinel. Similarly, the Δd_o in the mixed layer '$T_{Mg}^{I-t} + O_{Al}^{I-t} + T_{Mg}^{II-t}$' with a value of 3.1×10^{-4} is nearly the peak distortion on the AlO_6-octahedra, whereas the Δd_t with a value of 8.9×10^{-4} is the highest distortion on the MgO_4-tetrahedra. The Kagome layer within the hcp region of oxygen (Fig. 2a) exhibits the peak Δd_o of $4.6\text{x}10^{-4}$. As also seen on the figure, the polyhedral strain is not symmetric about the twin plane, with high strain/distortion concentrated in the mixed-cation layer (Fig. 2b). Such a strain distribution points to similar asymmetry in the energetics of inversion within the mixed-cation layer. The effect of the twin on the structure can also be seen in the mixed-cation layer wherein the $T_{Mg}^{1\text{-}t}$ and $O_{Al}^{1\text{-}t}$ layers nearly merge to form a single layer that is perpendicular to the [111]-direction. The merged layer, i.e. $T_{Mg}^{1\text{-}t} + O_{Al}^{1\text{-}t}$, is hereafter referred to as M-layer within the twinned hcp-region.

As also shown in Figure 2, the inversion energies for the formation of a single anti-site pair across different layers including those in the mixed-cation layer, i.e., the anti-site pair between the layers '$T_{Mg}^{II} - O_{Al}^{K-t}$' (marked as i-1), '$O_{Al}^{K-t} - T_{Mg}^{I-t}$' (marked as i-2), '$T_{Mg}^{I-t} - O_{Al}^{I-t}$' (marked as i-3), and '$O_{Al}^{I-t} - T_{Mg}^{II-t}$' (marked as i-4), are different but are more favored on the M-layer. The inversion energies are expressed as a decrease in the twin-formation energy in mJ/m^2. The twin-formation energy in pristine spinel without any cation inversion is 946 mJ/m^2. Driven by polyhedral distortions, the M-layer ($T_{Mg}^{I-t} + O_{Al}^{I-t}$) in the twinned region exhibits a stronger driving force for the cation-inversion than any other cation-layers. On the side of Kagome layer, as shown in Figure 2, the inversion involving the layers $T_{Mg}^{II} - O_{Al}^{K-t}$ is not favorable, leading to an increase in the twin-formation enthalpy by 16 mJ/m^2. In comparison, inversion on the other side involving mixed-cation layers is favorable, especially on the merged layer of $T_{Mg}^{I-t} + O_{Al}^{I-t}$, with a change in the twin formation enthalpy by -38 mJ/m^2. We note that in pristine spinel, the enthalpy of inversion is positive and unfavorable for the anti-site occupancies of Al and Mg.

A further examination of the degree of inversion on the merged cation-layer (layer '$T_{Mg}^{1\text{-}t} + O_{Al}^{1\text{-}t}$') in the vicinity of the twin plane is shown in Figure 3. With the employed 336-atom supercell, 1-, 2-, 3- and 4-pair inversions are possible within the layer. Based on the total number of cations within the layer, the inversions can be expressed as 25%, 50%, 75% and 100% and in terms of the inversion parameter x (in $Mg_{1-x}Al_{2-x}O_4$), within a 336-atom supercell, they represent 0.021, 0.042, 0.063, and 0.084 inversion, respectively. In addition, except at 100% inversion within

This is the peer-reviewed, final accepted version for American Mineralogist, published by the Mineralogical Society of America.
The published version is subject to change. Cite as Authors (Year) Title. American Mineralogist, in press.
DOI: https://doi.org/10.2138/am-2021-7874. http://www.minsocam.org/

this layer, several configurations are possible at each degree of inversion (Fig. 3). Clearly, based on the enthalpies, the M-layer within the twinned region prefers 100% inversion. In other words, relative to the (111) twin with no cation-disorder, the twin with inverted M-layer is more stable. The twin formation energy as a function of percentage inversion(p) on the M-layer yields a linear fit $\Delta H(p) = -3.6p + 957\ mJ/m^2$. As shown on Figure 4, in terms of structural relaxation that follows the inversion, the tetrahedral and polyhedral units in the mixed-cation layer (Fig. 4a) exhibits two important changes: (1) the AlO_4-tetrahedra shrink in volume by ~21% while MgO_6-octahedra expand in volume by 16% and (2) the Δd_o of the MgO_6-octahedra decreases by a four orders of magnitude, while the Δd_t of AlO_4-tetrahedra decreases by a factor of 3 (Fig. 4b). Thus, the inversion near the twin is a countervailing effect of the twin-induced distortions in the spinel lattice.

As a next step, we investigated the stability of the inverted M-layer at finite temperatures based on the free energies of inversion. The Gibbs free energy of inversion near the twin and within the layer is calculated by including the vibrational and configurational entropies, following the equation, $\Delta G_{inv}^{111}(T) = \Delta H_{inv}^{111} - T(\Delta S_{vib}^{111}(T) + S_{conf}^{111})$, where ΔH_{inv}^{111} and $\Delta S_{vib}^{111}(T)$ are the enthalpy and entropy changes due to the inversion near the twin, and S_{conf}^{111} is the configurational entropy due to the cation-disorder on the layer. Both the vibrational and configurational contributions to the entropy are positive at finite temperatures and favor the inversion, e.g., at 1000 K, the ΔS_{vib}^{111} at 100% inversion on the M-layer is 0.1316 mJ/m^2/K (Fig. 5a). As shown in Figure 5b, the $\Delta G_{inv}^{111}(T)$ is negative in the entire range of temperature for all degrees of inversion on the cation layer while it is most favorable for complete inversion with ΔH_{inv}^{111} and $\Delta S_{inv}^{111}(T)$ scaling favorably with the extent of inversion. The positive ΔS_{vib}^{111} indicates the softening of the bonds in the mixed-cation layer in the twinned region with the inversion. Such a softening is the net effect of changes in the Al-O and Mg-O bonds that result from the anti-site occupancies with the inversion. In summary, the twin-formation energy is lowered by the inversion on the cation layer, within the twinned region, with a complete inversion being the thermodynamically favored structure. In contrast, as mentioned earlier, within the pristine region, (i.e., the crystal region away from the twin plane) thermodynamics favor temperature-dependent limited inversion, which is negligible up to ~300 K. Such a difference in thermodynamics of inversion at and away from twins can lead to a distinct 'complexion' in terms of the local cation disorder near twins.

With thermodynamics favoring a complete inversion on the M-layer in the twinned region, at all temperatures, its evolution following (or accompanying) twinning is controlled by the inversion kinetics. The timescales for development of such twin complexion can be estimated based on the knowledge of inversion kinetics that is reported for the bulk. However, a direct use of rate constants of inversion obtained from the bulk, to predict the rate of inversion on a plane (i.e., the M-plane) that prefers complete disorder within the twinned region can lead to spurious estimate. In other words, especially with different thermodynamic potentials (i.e., the free energies) for disordering, the rates of inversion in the bulk and near the twin, as a function of inversion parameter could be different. Hence, we employed Ginzburg-Landau rate law to describe the evolution of disorder (Redfern et al. 1999) via inversion on the M-plane near the twin boundary.

$$\frac{dQ}{dt} = -\frac{\gamma \exp\left(-\frac{\Delta H^*}{RT}\right)}{2RT}\left(\frac{d\Delta G}{dQ}\right) \quad (2)$$

where Q (=1-3x/2) is an order parameter, x (in $Mg_{1-x}Al_{2-x}O_4$) is the inversion parameter as defined earlier, t is time, γ is a frequency factor, ΔH^* is the activation energy for disordering, and ΔG is the free energy change associated with disordering on the plane. The time required Δt (*=t-t_0)* for inversion near the (111) twin plane at a given temperature can be calculated by integrating the equation between Q_0 and Q (final). The time taken for complete inversion to occur on the M-plane after twinning, hence, is strongly dependent on temperature (Figure 6a). Figure 6a also depicts the free energies of twins with complete stable complexion and with no complexion, i.e., with the extent of inversion the same as in the bulk at any given temperature. The twins with same degree of inversion as in the bulk can be referred to as metastable twins. In addition, twins may have complexions that are in between the metastable twin and the completely stable twins. So, at any given temperature, their free energies can vary with the extent of inversion between the metastable and stable forms (Figure 6a).

Equation (2) is also used to calculate the inversion on the M-plane when a spinel is continuously cooled from the temperature where the twin occurred down to room temperature. Such a relationship can be used to deduce the temperature of twinning depending on the cooling rate of the twin-containing spinel and can be used as a thermochronometer. The $\frac{d\Delta G}{dQ}$ is obtained from the calculated $\Delta G_{inv}^{111}(x,T)$ (Figure 5b), and an activation energy of 260 kJ/mol for disordering is taken from literature (Kashii et al. 1999; Ma and Liu 2019). The frequency factor γ (1.354×10^9 1/s) is estimated for $MgFe_2O_4$ in an earlier study (Harrison 1997) of order/disorder

This is the peer-reviewed, final accepted version for American Mineralogist, published by the Mineralogical Society of America.
The published version is subject to change. Cite as Authors (Year) Title. American Mineralogist, in press.
DOI: https://doi.org/10.2138/am-2021-7874. http://www.minsocam.org/

kinetics and is also found to be applicable for $MgAl_2O_4$ (Redfern et al. 1999). Using such an estimate for γ while fitting their experimental data, the authors obtained an activation energy (230 kJ/mol) which is in good agreement with the literature value (260 kJ/mol) (Kashii et al. 1999; Ma and Liu 2019). The inversion during continuous cooling is calculated by a series of isothermal annealing steps with a small step size of 5 K and the contours of the extent of inversion, which is obtained on the M-plane of the spinel twin, are obtained between the temperature where it was twinned to room temperature (Figure 6b).

4. Discussion

As indicated by the thermodynamic driving force, the formation of a twin in a spinel grain leads to further inversion in its vicinity and temperature dictates the rate at which the local atomic disorder can occur. For example, following twinning, it takes 15,135 s at 973 K (776 s at 1073 K), for the complete inversion to occur near the twin plane. If the twinned spinel is not allowed sufficient time at the temperature where it is twinned (i.e., under isothermal conditions), a stable complexion will not develop, leading to metastable and incomplete inversions. Further, if twinning occurs at low temperatures ($T < \sim 700$ K), the sluggish kinetics, i.e. the longer timescales of inversion on the order of 10^9 s, can hinder the development of stable cationic-inversion in the mixed-cation layer (Figure 6a). However, at high temperatures ($T \geq \sim 1473$ K) the stable cationic-inversion follows the developing twin quickly with timescales on the order of seconds to microseconds and will be retained when cooled to low temperatures. An important implication for growth twins is that, in view of their high-temperature origin, they exhibit the characteristic stable inversion as depicted in Figure 4. In the case of deformation twins, depending on the twinning temperature, it is possible to get different twin complexions. Thus, it is clear that the interplay between thermodynamics and the kinetics of inversion can lead to stable and metastable inversions near the twin boundary.

The relationship between inversion and twinning has important implications for different areas of study ranging from materials physics to earth and planetary science. In the case of the former, the knowledge of the evolution of twin-associated inversion is crucial to describe the dislocation dynamics in spinel. The dislocation dissociation and glide kinetics are directly dependent on the twin-formation energies and hence on the extent and rate of inversion that can accompany the

twinning process. In the case of the latter, extent of inversion could shed light into high-temperature processes that affected MAS and other materials in, e.g., the solar protoplanetary disk. More specifically, the extent of inversion near the twin plane, if quantified in meteoritic MAS, can be used as a thermochronometer. The partial and metastable configurations compared to complete and stable configurations of disorder can be denoted as two distinct complexions generated at low and high temperatures, respectively. In the case of CAI spinels, the temperature at which twinning occurred and the time elapsed after the formation of the twin are the two important factors that dictate the extent of inversion, i.e., the complexion at the twin. Hence, if the extent of inversion near the twin (relative to the bulk) can be measured, it is possible to infer the twinning temperature for a given cooling rate after the twinning. For extremely slow cooling rates on the order of 1 K/hr, the twins exhibit the same inversion as in the bulk if twinning occurred at $T < 737$ K. However, for a faster cooling rate on the order of 1000 K/hr, which was reported for some CAIs (Stolper and Paque 1986), the twins, relative to the bulk, will have no complexion if twinning occurred at $T < 878$ K. Similarly, for cooling rates of 1 K/hr, if a CAI spinel exhibits stable and complete inversion, it points to a twinning temperature of > 917 K. Further, as presented in the proposed thermochronometer, the partial and incomplete twin complexions can precisely help deduce the twinning temperature for a given cooling rate. For example, a 70% inversion on the M-plane of the twin boundary would indicate that twinning must have occurred at 960 K if the MAS was cooled at 10 K/hr after it twinned. Hence, if the extent of inversion can be determined in MAS at the atomic scale, by employing characterization tools such as aberration-corrected transmission electron microscopy, then such information could be used as a quantitative constraint on its thermal history. The developed thermochronometer can also be extended for spinels with other alloying elements such as Fe, Ti and V. Similarly, such twin boundary complexions can also evolve as a function of pressure and can be extended to develop barometers for geological purposes.

5. Implications

Twinning in $MgAl_2O_4$ spinel on the (111) plane leads to polyhedral strains and distortions that are asymmetric about the twin plane. As a consequence, the twins exhibit cation inversion that is not symmetric. Within the twinned region of the crystal, complete inversion within the mixed-cation layer is thermodynamically favorable and stable over the entire temperature range of twin formation. These findings, in conjunction with kinetics of inversion, point to the temperature-

dependent evolution of stable and metastable cation disorder near the twins. A thermochronometer based on the twin complexions, for MAS, is developed. Atomic-scale characterization of extent of cation disorder associated with twins, hence, can help deduce the thermal condition under which the faults formed. In CAI assemblages, the cooling rates deduced from other microstructural features if used in conjunction with the developed thermochronometer can constrain the possible twin complexions in CAI-spinels. As a result, twins in CAI-spinels can be used as markers of nebular processes such as flash heating, thermal metamorphism and shock metamorphism.

Acknowledgements

Research supported by the NASA Emerging Worlds Program (NNX15AJ22G and 80NSSC19K0509). Resources supporting this work were provided by the NASA High-End Computing (HEC) Program through the NASA Advanced Supercomputing (NAS) Division at Ames Research Center. The authors also acknowledge the high-performance computing facility at the University of Arizona.

References

Amelin, Y., Krot, A.N., Hutcheon, I.D., and Ulyanov, A.A. (2002) Lead isotopic ages of chondrules and calcium-aluminum-rich inclusions. Science, 297, 1678–1683.

Biagioni, C., and Pasero, M. (2014) The systematics of the spinel-type minerals: An overview. American Mineralogist, 99, 1254–1264.

Birch, F. (1947) Finite elastic strain of cubic crystals. Physical Review, 71, 809–824.

Birch, F. (1978) Finite strin isotherm and velocities for single-crystal and polycrystalline NaCl at high-pressures and 300 K. Journal of Geophysical Research, 83, 1257–1268.

Bosi, F., Skogby, H., Fregola, R.., and Halenius, U. (2016) Crystal chemistry of spinels in the system MgAl2O4 -MgV2O4 -Mg2VO4. American Mineralogist, 101, 580–586.

Brearely, A.J., and Jones, R.H. (1998) Planetary materials. (J.J. Papike, Ed.).

Brownlee, D. (2014) The stardust mission: Analyzing samples from the edge of the solar system. Annual Review of Earth and Planetary Sciences, 42, 179–205.

Ciesla, F.J. (2007) Outward transport of high-temperature materials around the midplane of the solar nebula. Science, 318, 613–615.

Ciesla, F.J. (2009) Dynamics of high-temperature materials delivered by jets to the outer solar nebula. Meteoritics and Planetary Science, 44, 1663–1673.

Connelly, J.N., Bizzarro, M., Krot, A.N., Nordlund, Å., Wielandt, D., and Ivanova, M.A. (2012) The absolute chronology and thermal processing of solids in the solar protoplanetary disk. Science, 338, 651–655.

Dugdale, J.S., and MacDonald, D.K.C. (1953) The thermal expansion of solids. Physical Review, 89, 639–648.

Ganesh, I. (2013) A review on magnesium aluminate (MgAl2O4) spinel: Synthesis, processing

and applications. International Materials Reviews, 58, 63–112.
Goncalves-Ferreira, L., Redfern, S.A.T., Artacho, E., and Salje, E.K.H. (2008) Ferrielectric twin walls in CaTiO3. Physical Review Letters, 101, 1–4.
Harrison, R.J. (1997) Magnetic properties of the magnetite-spinel solid solution. University of Cambridge.
Hornstra, J. (1960) Dislocations, stacking faults and twins in the spinel structure. Journal of Physics and Chemistry of Solids, 15, 311–323.
Kashii, N., Meakawa, H., and Hinatsu, Y. (1999) Dynamics of the cation mixing of MgAl2O4 and ZnAl2o4 spinel, 82, 1844.
Kresse, G., and Furthmüller, J. (1996) Efficient iterative schemes for ab initio total-energy calculations using a plane-wave basis set. Physical Review B - Condensed Matter and Materials Physics, 54, 11169–11186.
Krivanek, O.L., Chisholm, M.F., Nicolosi, V., Pennycook, T.J., Corbin, G.J., Dellby, N., Murfitt, M.F., Own, C.S., Szilagyi, Z.S., Oxley, M.P., and others (2010) Atom-by-atom structural and chemical analysis by annular dark-field electron microscopy. Nature, 464, 571–574.
Ma, Y., and Liu, X. (2019) Kinetics and thermodynamics of Mg-Al disorder in MgAl2O4-Spinel: A review. Molecules, 24, 1–25.
MacPherson, G.J. (2014) Calcium–Aluminum-Rich Inclusions in Chondritic Meteorites. In H.D. Holland and K.K.B.T. Turekian, Eds., pp. 139–179. Elsevier, Oxford.
Méducin, F., Redfern, S.A.T., Le Godec, Y., Stone, H.J., Tucker, M.G., Dove, M.T., and Marshall, W.G. (2004) Study of cation order-disorder in MgAl2O4 spinel by in situ neutron diffraction up to 1600 K and 3.2 GPa. American Mineralogist, 89, 981–986.
Navrotsky, A., and Kleppa, O.J. (1967) The thermodynamics of cation distributions in simple spinels. Journal of Inorganic and Nuclear Chemistry, 29, 2701–2714.
O'Keefe, M., and Hyde, B.G. (1997) Crystal Structures, Vol. 1, Patterns and Symmetry. Mineralogical Magazine, 61, 741–742.
O'Neill, H.S.C., and Navrotsky, A. (1984) Cation distributions and thermodynamic properties of binary spinel solid solutions. American Mineralogist, 69, 733–753.
Parisi, F., Lenaz, D., Princivalle, F., and Sciascia, L. (2014) Ordering kinetics in synthetic Mg(Al,Fe3+)2O4 spinels: Quantitative elucidation of the whole Al-Mg-Fe partitioning, rate constants, activation energies. American Mineralogist, 99, 2203–2210.
Pennycook, S.J. (2017) The impact of STEM aberration correction on materials science. Ultramicroscopy, 180, 22–33.
Perdew, J.P., and Zunger, A. (1981) Self-interaction correction to density-functional approximations for many-electron systems. Physical Review B, 23, 5048–5079.
Perdew, J.P., Burke, K., and Ernzerhof, M. (1996) Generalized Gradient Approximation Made Simple. Phys. Rev. Lett., 77, 3865–3868.
Rasmussen, M.K., Foster, A.S., Hinnemann, B., Canova, F.F., Helveg, S., Meinander, K., Martin, N.M., Knudsen, J., Vlad, A., Lundgren, E., and others (2011) Stable Cation Inversion at the MgAl2O4 (100) Surface. Phys. Rev. Lett., 107, 36102.
Redfern, S.A.T., Harrison, R.J., O'Neill, H.S.C., and Wood, D.R.R. (1999) Thermodynamics and kinetics of cation ordering in natural and synthetic Mg(Al,Fe3+)2O4 spinels from in situ high-temperature X-ray diffraction. American Mineralogist, 84, 299–310.
Slater, J.C. (1939) Introduction to chemical physics. McGraw-Hill, Newyork.
Stolper, E., and Paque, J.M. (1986) Crystallization sequences of Ca-Al-rich inclusions from Allende: The effects of cooling rate and maximum temperature. Geochimica et

Cosmochimica Acta, 50, 1785–1806.
Uberuaga, B.P., and Perriot, R. (2020) Spatially-varying inversion near grain boundaries in MgAl2O4 spinel. RSC Advances, 10, 11737–11742.

Figure Captions

Figure 1. Polyhedral model of pristine $MgAl_2O_4$-spinel with no cation-inversion as viewed along [10-1]. The oxygen atoms at the corners of tetrahedral and octahedral units are not shown for clarity. O^K_{Al} and O^I_{Al} stand for Al in the octahedral sites in the Kagome layer and in the mixed-cation layers, respectively. T^I_{Mg} and T^{II}_{Mg} stand for Mg in tetrahedral sites, as two different layers within the mixed-cation layer. ABCABC… stacking represents the cubic close packing of oxygen in the spinel.

Figure 2. Polyhedral model of MAS twin and the polyhedral distortion parameter. (a) (111) twin in $MgAl_2O_4$-spinel with no cation inversion. The oxygen atoms at the corners of tetrahedral and octahedral units are not shown for clarity. The local ACA packing within the ABCABC… stacking sequence of oxygen sub-lattice is the spinel twin. I-refers to mixed cation layers and K refers to Kagome layer. The inversions (marked as i-1 to i-4) change the twin- formation energy by: +16 mJ/m^2 for i-1; -10 mJ/m^2 for i-2; -29 mJ/m^2 for i-3; and -38 mJ/m^2 for i-4. (b) The octahedral (green) and tetrahedral (red) distortion parameters in each layer on either side of the twin plane.

Figure 3. Enthalpies of twin formation as a function of extent of inversion on the merged layer (marked as $T_{Mg}^{I-t} + O_{Al}^{I-t}$ in Figure 2a) within the twinned (hcp) region. Each black dot on the plot corresponds to energies at a given percentage of inversion and configuration. At each percentage of inversion, several atomic configurations (inset) are possible; at 25% and 50% inversions only some of the calculated configurations are shown. Solid red circles correspond to Mg and solid blue circles correspond to Al on the merged layer.

Figure 4. Polyhedral model of MAS twin and the polyhedral distortion parameter. (a) Stable atomic structure of (111) twin with complete inversion on the mixed cation-layer within the twinned ACA region. The oxygen atoms at the corners of tetrahedral and octahedral units are not shown for clarity. The marked mixed-cation layer in the twinned (ACA) region has Mg and Al atoms in the octahedral and tetrahedral sites, respectively. (b) The octahedral (green) and tetrahedral (red) distortion parameters in each layer on either side of the twin plane.

This is the peer-reviewed, final accepted version for American Mineralogist, published by the Mineralogical Society of America.
The published version is subject to change. Cite as Authors (Year) Title. American Mineralogist, in press.
DOI: https://doi.org/10.2138/am-2021-7874. http://www.minsocam.org/

Figure 5. Thermodynamic driving force, expressed as the decrease in twin formation energy, for cation-inversion on the merged layer (marked as $T_{Mg}^{I-t} + O_{Al}^{I-t}$) in the twinned region. (a) Changes in vibrational entropy associated with the extent of cation-inversion. (b) Changes in twin formation energy with the extent of cation-inversion.

Figure 6. (a) Timescales for Al/Mg-inversion on the merged layer (referred as M-layer: $T_{Mg}^{I-t} + O_{Al}^{I-t}$) within the twinned region. The time taken for inversion is calculated by integrating the Ginzburg-Landau rate law at different temperatures under isothermal conditions. The twin free energies with stable and metastable inversions (i.e. with extent of inversion same as in bulk) as a function of temperature are also shown. (b) Contours of the extent of inversion that are obtained at room temperature on the M-layer as a function of the temperature at which twinning occurred and the cooling rate.

Figure 1

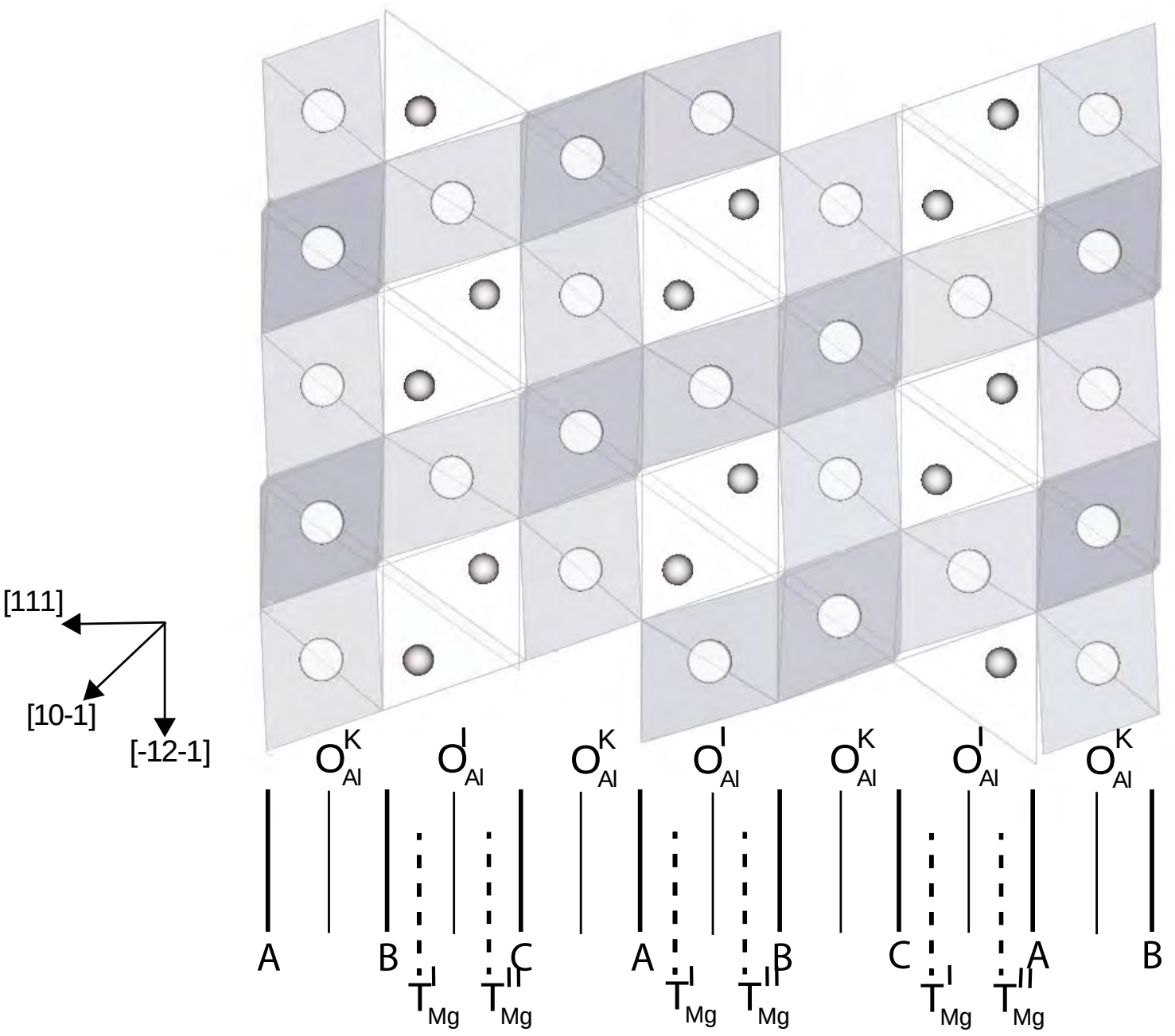
[111]
[10-1]
[-12-1]
O^K_{Al}
O^I_{Al}
O^K_{Al}
O^I_{Al}
O^K_{Al}
O^I_{Al}
O^K_{Al}
A
B
C
A
B
C
A
B
T^I_{Mg}
T^{II}_{Mg}
T^I_{Mg}
T^{II}_{Mg}
T^I_{Mg}
T^{II}_{Mg}

Figure 2

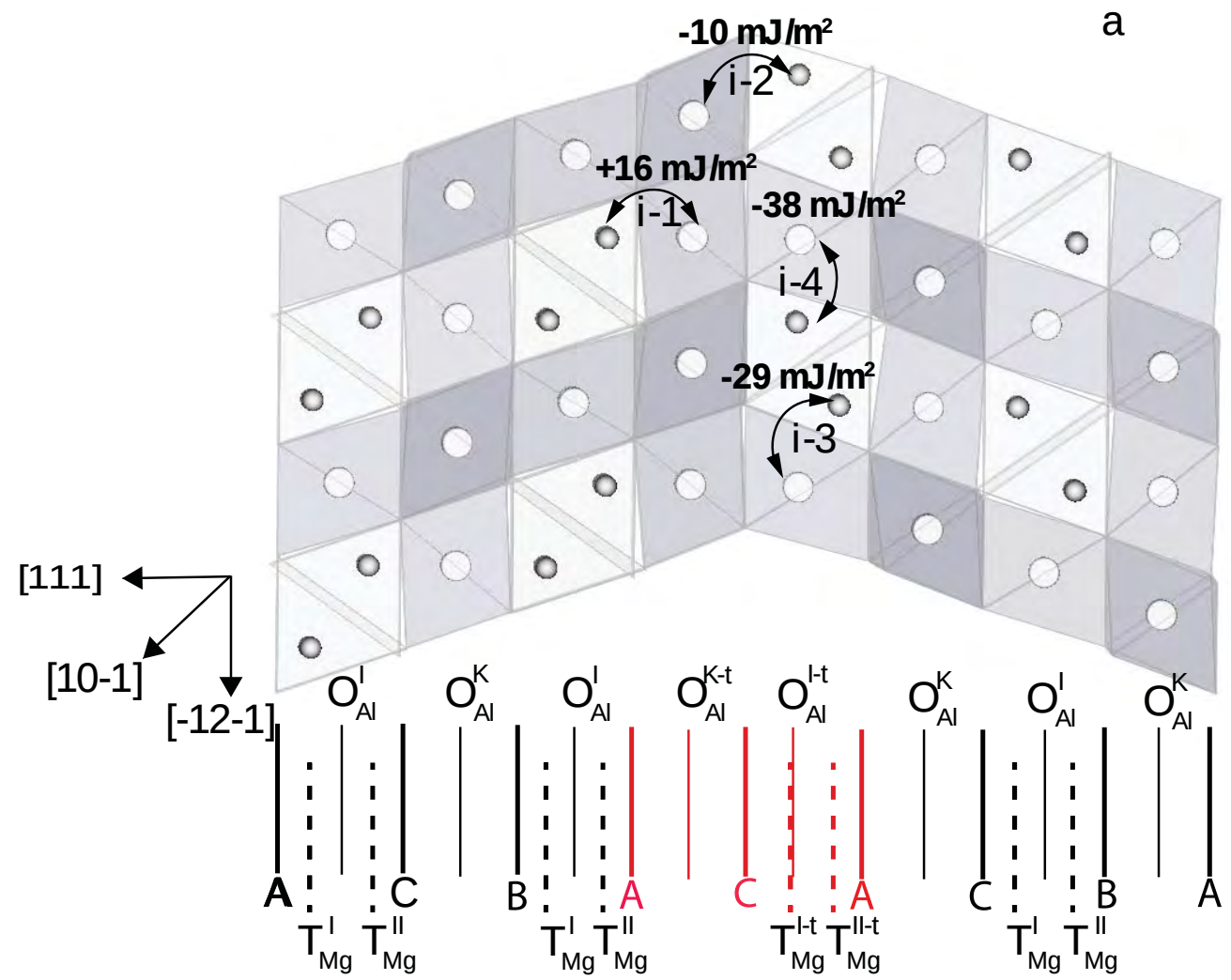
a
-10 mJ/m²
i-2
+16 mJ/m²
i-1
-38 mJ/m²
i-4
-29 mJ/m²
i-3
[111]
[10-1]
[-12-1]
A
C
B
A
C
A
C
B
A

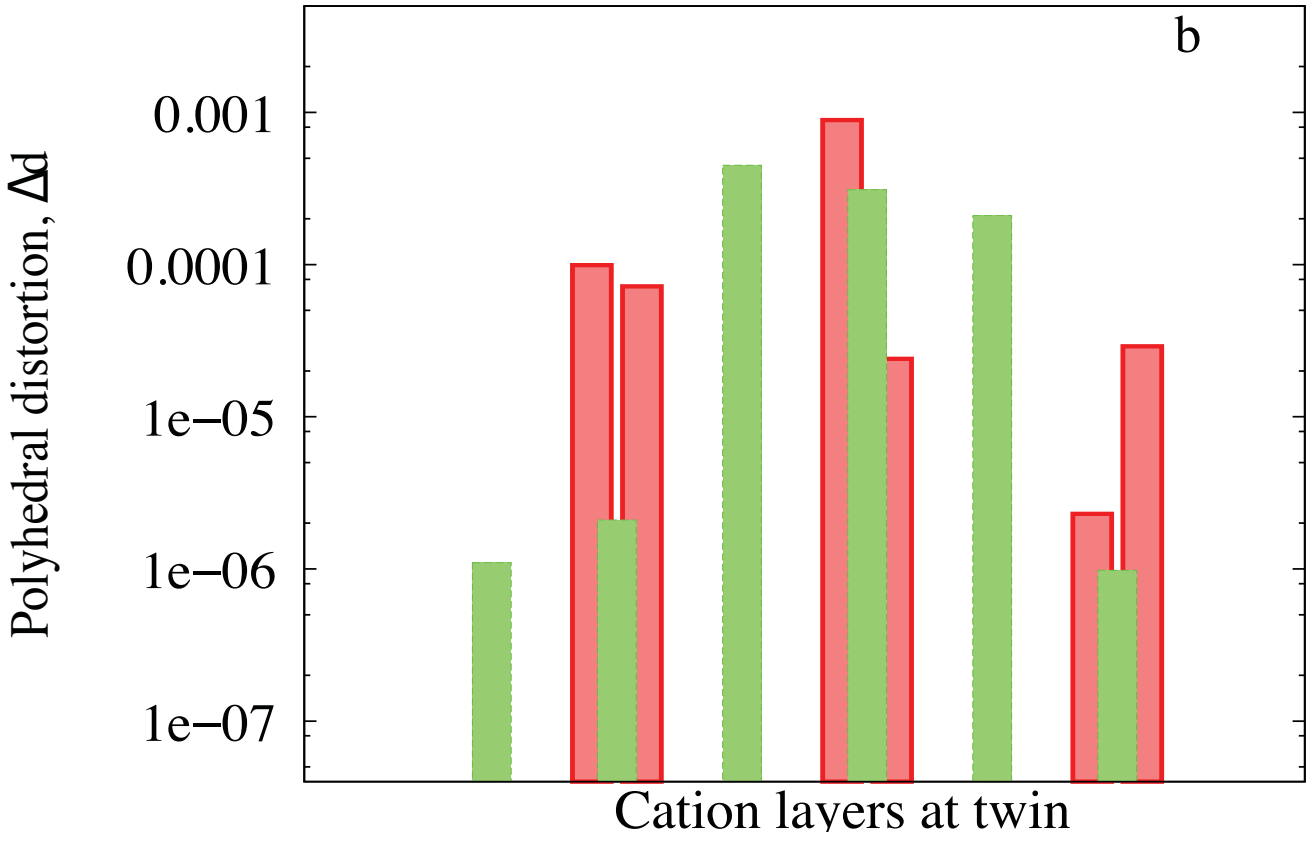
b
Polyhedral distortion, Δd
0.001
0.0001
1e−05
1e−06
1e−07
Cation layers at twin

Figure 3

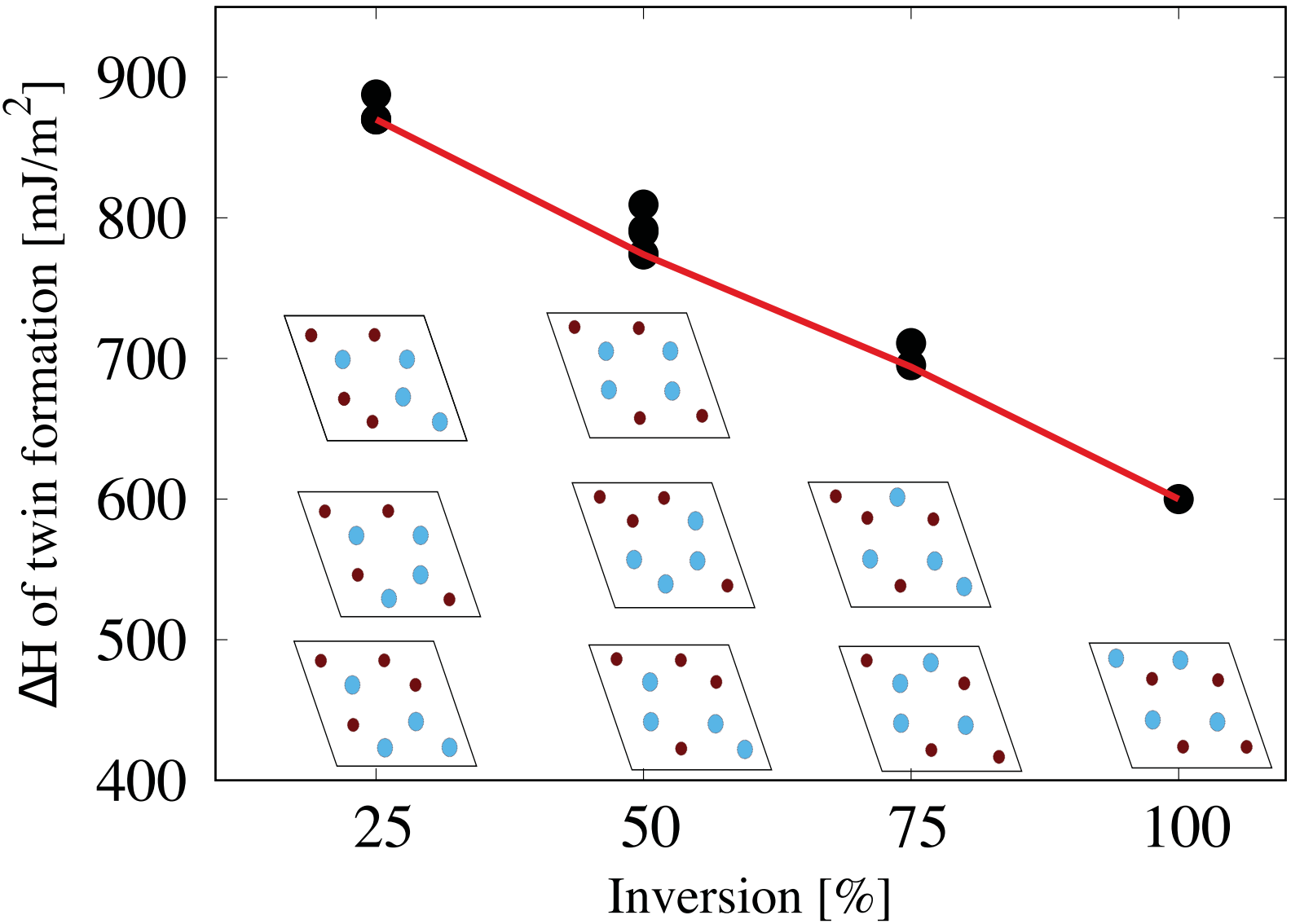
900
800
700
600
500
400
ΔH of twin formation [mJ/m2]
25
50
75
100
Inversion [%]

Figure 4

a

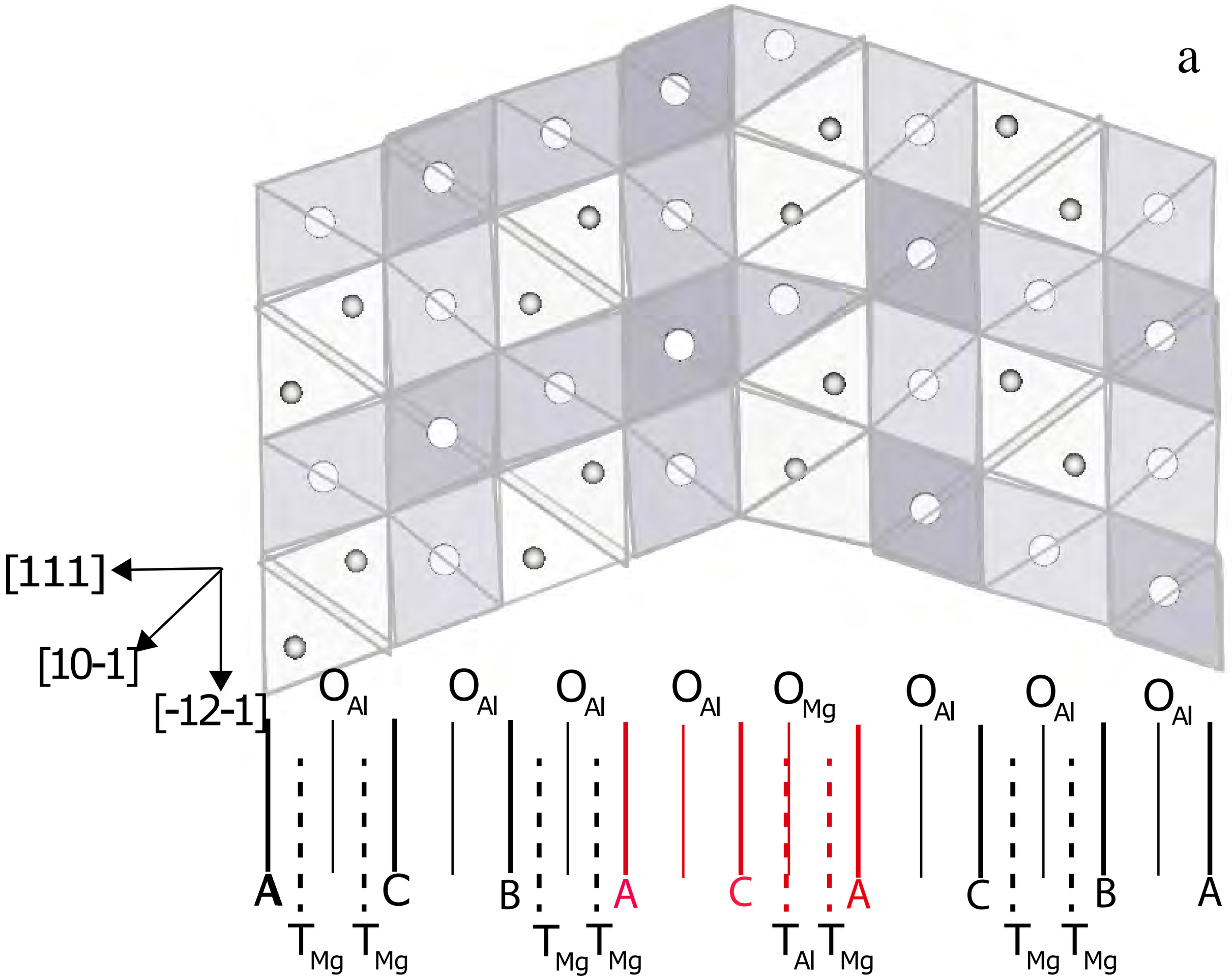
[111]
[10-1]
[-12-1]
O Al
O Al
O Al
O Al
O Mg
O Al
O Al
O Al
A
C
B
A
C
A
C
B
A
T Mg T Mg
T Mg T Mg
T Al T Mg
T Mg T Mg

b

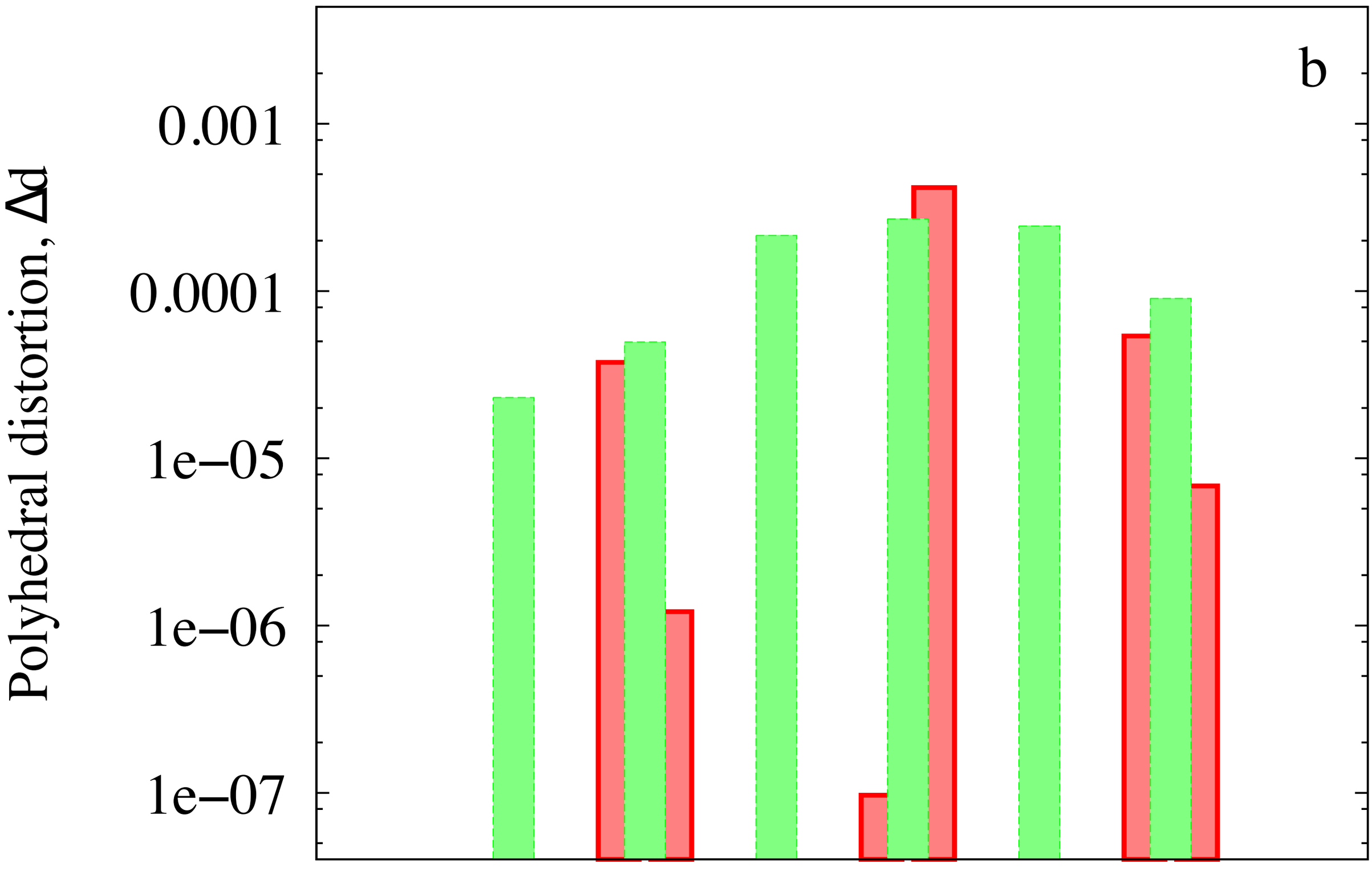
0.001
0.0001
1e–05
1e–06
1e–07
Polyhedral distortion, Δd
Cation layers at twin

Figure 5

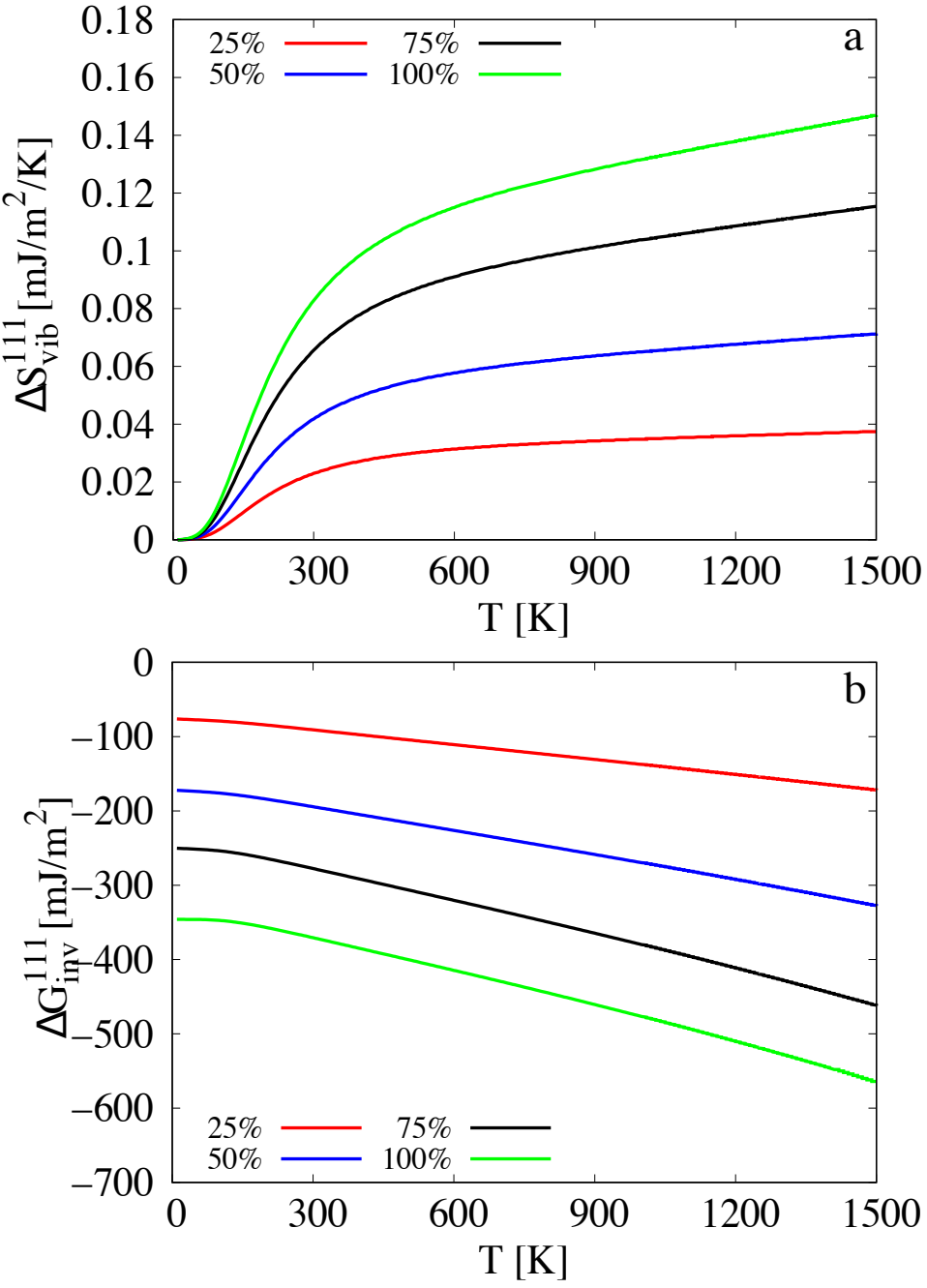
a
25%
50%
75%
100%
ΔS^{111}_{vib} [mJ/m^2/K]
0.18
0.16
0.14
0.12
0.1
0.08
0.06
0.04
0.02
0
0
300
600
900
1200
1500
T [K]
b
ΔG^{111}_{inv} [mJ/m^2]
0
−100
−200
−300
−400
−500
−600
−700
25%
50%
75%
100%
0
300
600
900
1200
1500
T [K]

Figure 6

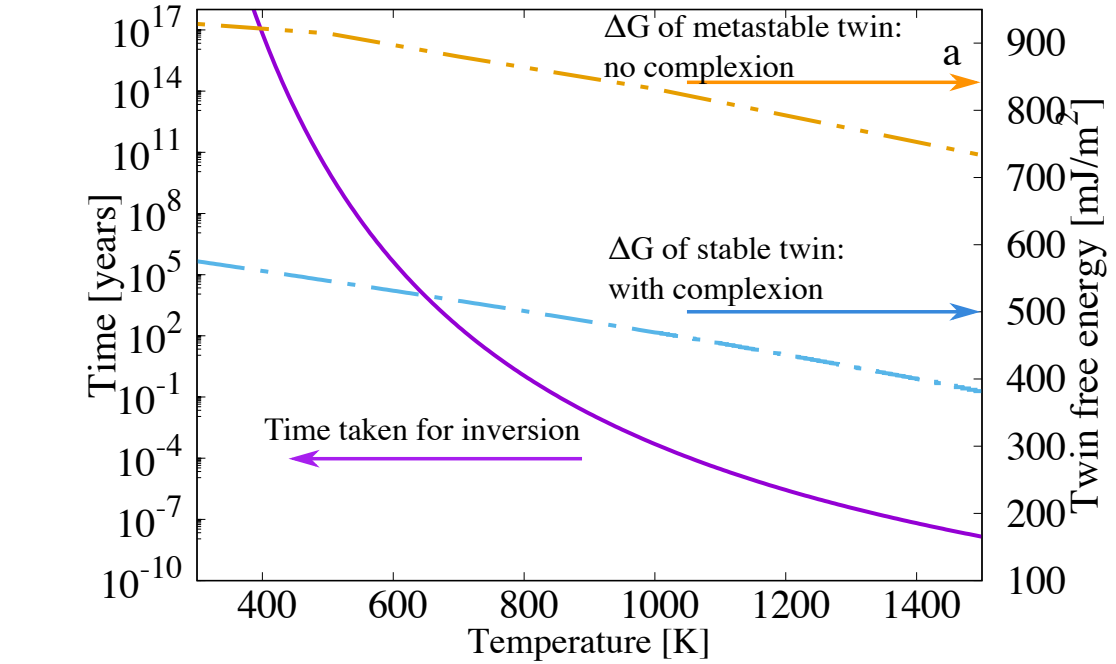
ΔG of metastable twin:
no complexion
a
ΔG of stable twin:
with complexion
Time taken for inversion
Time [years]
Twin free energy [mJ/m²]
Temperature [K]
10^17
10^14
10^11
10^8
10^5
10^2
10^-1
10^-4
10^-7
10^-10
900
800
700
600
500
400
300
200
100
400
600
800
1000
1200
1400

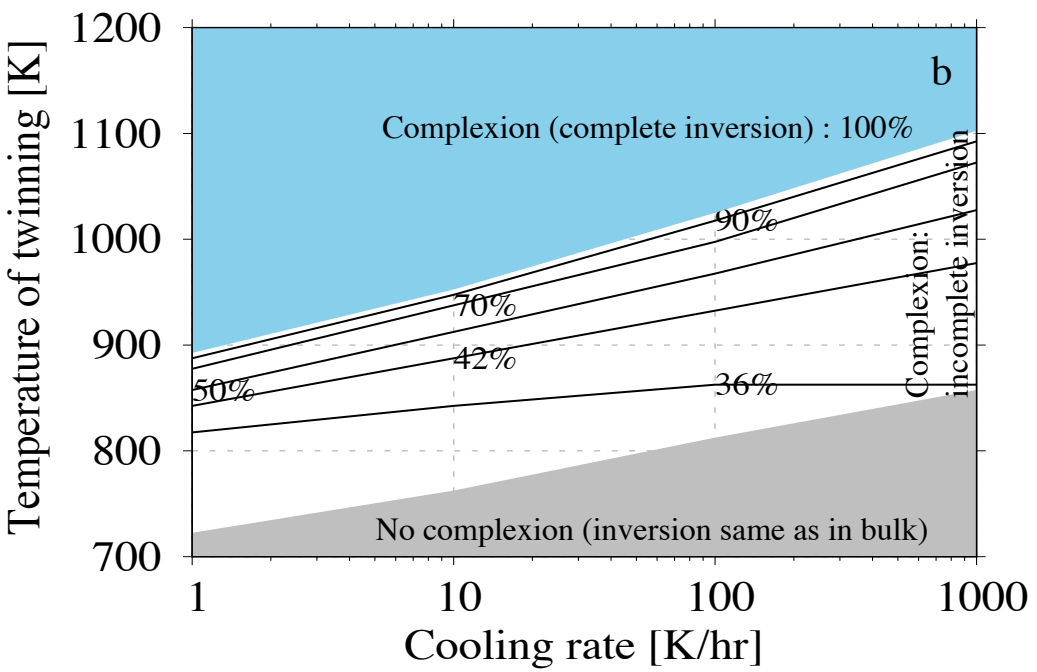
b
Complexion (complete inversion) : 100%
90%
70%
42%
50%
36%
Complexion: incomplete inversion
No complexion (inversion same as in bulk)
Temperature of twinning [K]
Cooling rate [K/hr]
1200
1100
1000
900
800
700
1
10
100
1000